

Article

# Transcriptomic Profiling of Pomegranate Provides Insights into Salt Tolerance

Cuiyu Liu <sup>1,2</sup>, Yujie Zhao <sup>1,2</sup>, Xueqing Zhao <sup>1,2</sup> , Jinping Wang <sup>1,2</sup>, Mengmeng Gu <sup>3,\*</sup>  and Zhaohu Yuan <sup>1,2,\*</sup>

<sup>1</sup> Co-Innovation Center for Sustainable Forestry in Southern China, Nanjing Forestry University, Nanjing 210037, China; liucuiyu88@gmail.com (C.L.); z1184985369@163.com (Y.Z.); zhaoxq402@163.com (X.Z.); wangjp0304@163.com (J.W.)

<sup>2</sup> College of Forestry, Nanjing Forestry University, Nanjing 210037, China

<sup>3</sup> Department of Horticultural Sciences, Texas A&M AgriLife Extension Service, College Station, TX 77843-2134, USA

\* Correspondence: mgu@tamu.edu (M.G.); zhyuan88@hotmail.com (Z.Y.); Tel.: +1-979-845-8545 (M.G.); +86-025-8542-7056 (Z.Y.)

Received: 17 October 2019; Accepted: 24 December 2019; Published: 27 December 2019



**Abstract:** Pomegranate (*Punica granatum* L.) is widely grown in arid and semi-arid soils, with constant soil salinization. To elucidate its molecular responses to salt stress on mRNA levels, we constructed 18 cDNA libraries of pomegranate roots and leaves from 0 (controls), 3, and 6 days after 200 mM NaCl treatment. In total, we obtained 34,047 genes by mapping to genome, and then identified 2255 DEGs (differentially expressed genes), including 1080 up-regulated and 1175 down-regulated genes. We found that the expression pattern of most DEGs were tissue-specific and time-specific. Among root DEGs, genes associated with cell wall organization and transmembrane transport were suppressed, and most of metabolism-related genes were over-represented. In leaves, 41.29% of DEGs were first suppressed and then recovered, including ions/metal ions binding-related genes. Also, ion transport and oxidation-reduction process were restricted. We found many DEGs involved in ABA, Ca<sup>2+</sup>-related and MAPK signal transduction pathways, such as ABA-receptors, Ca<sup>2+</sup>-sensors, MAPK cascades, TFs, and downstream functional genes coding for HSPs, LEAs, AQPs and PODs. Fifteen genes were selected to confirm the RNA-seq data using qRT-PCR. Our study not only illuminated pomegranate molecular responses to salinity, but also provided references for selecting salt-tolerant genes in pomegranate breeding processes.

**Keywords:** pomegranate; salt stress; transcriptome; tissue-specific; signaling transduction pathways; transcription factors

## 1. Introduction

Soil salinization is defined as the excess or deposition of salt ions in land, which may interfere with plant growth. With the aggravation of soil salinization, it has become a considerable threat to healthy and sustainable development of worldwide agriculture [1]. Approximate 20% of the global cultivated lands and 50% of the irrigated lands are affected by salinity [2]. Plants exposed to saline conditions mainly suffer from osmotic stress, ion toxicity, and nutrient deficiency [3,4]. Consequently, all of the significant processes involved in plant growth and development, such as photosynthesis, protein synthesis, energy conversion and ion balance, could be affected by salinity [5]. The effects of salinity depend, not only on species, genotypes, and the age of plants, but also on the duration and intensity of stress [6]. Meanwhile, plants can adapt to saline environment with following strategies: (1) Efficiently controlling the uptake, transport, and compartmentalization of toxic ions;

(2) synthesis of osmoregulation substances and activation of antioxidant enzymes; (3) formation of unique morphological structures, such as succulent leaves, salt glands and bladders [7,8].

Plant salt-tolerance is a quantitative trait controlled by multiple genes [4]. Using transcriptomic analysis, researchers can identify the salt-related genes with differential and temporal expression patterns in plants, and provide a clear picture of transcripts in response to salt stress. These salt-related genes are identified and categorized into two types according to the functions of proteins [4]. The first type is the effector code the functional proteins, which are directly involved in the physiological and biochemical responses to salt stress in plants. These proteins include the superoxide dismutase (SOD) [9], ascorbate peroxidase (APX) [10], high-affinity potassium transporter (HKT) [11],  $\text{Na}^+/\text{H}^+$  antiporter (NHX) [12], aquaporin (AQP) [13], late embryogenesis abundant (LEA) [14], and  $\text{H}^+$ -ATPase (VHA) [15], etc. The second type is regulator that involved in regulating the expressions of genes and the signal transduction pathways, such as transcription factors (TFs) and various kinases [16]. These well-characterized TFs include Apetala2/ethylene response factor (AP2/ERF), dehydration-responsive element-binding protein/C-repeat binding factor (DREB/CBF), WRKY, NAC, basic leucine zipper (bZIP), MYB, and basic helix-loop-helix (bHLH) family members [4]. These genes regulate the expressions of downstream genes via various ways, then may influence the plants salt-tolerance eventually [17]. Under salt stress, many signaling transduction pathways are stimulated in plants, such as  $\text{Ca}^{2+}$ -related, abscisic acid (ABA), and mitogen-activated protein kinase (MAPKs), as well as the crosstalk networks among them, which play crucial roles in responses to salt stress [4,18].

Pomegranate (*Punica granatum* L.) is an emerging commercial fruit tree of the Lythraceae family [19]. In recent years, pomegranate is increasingly popular with extensive usage of its fruits and products, and it is considered a 'super fruit' with high nutritional and medicinal values [20]. The species is widely grown in arid and semiarid regions where the availability and irrigation of saline water are significant issues [21]. Thus, it is important to explore pomegranate potential salt tolerance. Considerable research has been done on pomegranate physiological and biochemical responses to salinity, especially on its growth, ion balance, osmoregulation, and the scavenging of reactive oxygen species (ROS) [22–24]. In this study, we used roots and leaves of a pomegranate cultivar 'Taishanhong' with whole genomic sequence released to perform deep transcriptome sequencing and then demonstrate a global representation of potential candidate genes under salt stress. We aim to unravel the fundamental molecular mechanisms in pomegranate underlying the responses to salt stress.

## 2. Materials and Methods

### 2.1. Plant Growth and Stress Treatments

Uniform rooted cuttings of pomegranate ('Taishanhong') were obtained from the Pomegranate Repository of Nanjing Forestry University, China. They were grown in plastic pots (2.5 L) containing medium (1:1 by volume of perlite and peat,  $1.5 \pm 0.1$  Kg) in a climate controlled chamber for six months (14 h light 26 °C/10 h dark 22 °C), and fertigated weekly with  $\frac{1}{2}$  Hoagland's solution [25].

At the beginning of experiment, forty-five plants were randomly selected and divided into 3 groups, fifteen plants per group. The roots and leaves of the first group of plants were harvested as control samples (T0R and T0L). The other two groups of plants were fertigated once with 500 mL of  $\frac{1}{2}$  Hoagland's solution containing 200 mM NaCl. A saucer was placed under each container to collect leachate solution during the experiment period. The roots and leaves of the second group of plants on day 3 (T1R and T1L) and the third group of plants on day 6 (T2R and T2L) were harvested later. There was not visible difference between the treated and untreated plant (Figure S1). Samples from five plants in the same group were pooled together as a replicate due to the small amount of biomass. All samples were immediately frozen in liquid nitrogen and then stored at  $-80$  °C.

## 2.2. RNA Preparation, cDNA Library Construction and Sequencing

Total RNA was extracted from pomegranate roots and leaves using the Total RNA Kit (Tiangen, Beijing, China) according to the manufacturer's instructions. RNA purity, concentration and integrity were checked using the NanoPhotometer<sup>®</sup> spectrophotometer (IMPLEN, Westlake Village, CA, USA), Qubit<sup>®</sup> RNA Assay Kit in Qubit<sup>®</sup> 2.0 Fluorometer (Life Technologies, Carlsbad, CA, USA) and the RNA Nano 6000 Assay Kit of the Agilent Bioanalyzer 2100 (Agilent Technologies, Santa Clara, CA, USA), respectively.

A total amount of 3 µg RNA per sample was used as input material for the RNA sample preparations. Sequencing libraries were generated using NEB Next<sup>®</sup> Ultra<sup>™</sup> RNA Library Prep Kit for Illumina<sup>®</sup> (NEB, Ipswich, MA, USA) following manufacturer's recommendations and index codes were added to attribute sequences to each sample. The RNA samples were concentrated using magnetic oligo (dT) beads and then broken into short fragments using an RNA Fragmentation buffer (NEB Next First Strand Synthesis Reaction Buffer (5X), Ambion, Austin, TX, USA). The first-strand cDNA was synthesized using random hexamer primer and M-MuLV Reverse Transcriptase (RNase H-). Second-strand cDNA was synthesized subsequently using DNA Polymerase I and RNase H. After adenylation of 3' ends of DNA fragments, NEB Next Adaptor with hairpin loop structure were ligated to prepare for hybridization. The cDNA fragments with suitable lengths (150~200 bp) were purified with AMPure XP system (Beckman Coulter, Beverly, MA, USA) to construct the final cDNA libraries. Then 3 µL USER Enzyme (NEB, USA) was used with size-selected, adaptor-ligated cDNA at 37 °C for 15 min followed by 5 min at 95 °C before PCR. Next, the selected cDNA fragments were enriched via PCR with Phusion High-Fidelity DNA polymerase, Universal PCR primers and Index (X) Primer. PCR products were purified with AMPure XP system and the cDNA libraries were assessed on the Agilent Bioanalyzer 2100 system. Finally, the clustering of the index-coded samples was performed on a cBot Cluster Generation System using TruSeq PE Cluster Kit v3-cBot-HS (Illumina, Inc., San Diego, CA, USA) according to the manufacturer's instructions. After cluster generation, the library preparations were sequenced on an Illumina HiSeq 4000 platform (Illumina, Inc., San Diego, CA, USA) and 150 bp paired-end reads were generated.

## 2.3. Sequence Assembly

Low quality reads and reads containing adapter and ploy-N were filtered by NGS QC ToolKit [26] from raw reads. At the same time, Q20, Q30, GC-content and sequence duplication level of the clean data were calculated. All the downstream analyses were based on clean data with high quality. The clean data from all 18 libraries were separately mapped to the pomegranate genome assembly (ASM220158v1) using HISAT2 software [27]. StringTie [28] was used to construct and identify both known and novel transcripts from HISAT2 alignment results. StringTie was also used to count the reads numbers mapped to each gene. After that, FPKM (Fragments Per Kilobase of exon per million fragments Mapped) were calculated based on the length of the gene and reads count mapped to this gene [27].

## 2.4. Identification and Functional Annotation of DEGs

All genes were compared against various protein databases by BLASTX, including the Nr (NCBI non-redundant protein sequences); Pfam (Protein family); KOG/COG (Clusters of Orthologous Groups of proteins), and Swiss-Prot (A manually annotated and reviewed protein sequence database) with an E-value cut-off of  $10^{-5}$ . Then genes with the best BLAST hit (the highest score) were chosen along with their protein functional annotations. DESeq and Q-value were employed to evaluate the differential expression genes (DEGs) between controls and treatments. The false discovery rate (FDR) and  $\log_2FC$  (log of fold change) were calculated for all genes, and only transcripts with  $FDR < 0.05$  and  $|\log_2(\text{fold change})| \geq 1$  were considered as DEGs. To annotate the DEGs with gene ontology (GO) terms, the Nr BLAST results were imported into the Blast2GO program [29]. To examine the expression

patterns of DEGs, the expression data from roots and leaves (T0, T1 and T2) were normalized to 0,  $\log_2(T1/T0)$ ,  $\log_2(T2/T0)$ , and then clustered by Short Time-series Expression Miner software (STEM) separately, using a FDR correction method and  $p$ -value  $\leq 0.05$  as the cutoff [30]. The results of GO annotations in each pattern were enriched and refined using TBtools v0.6652 (Toolbox for Biologists, <https://github.com/CJ-Chen/TBtools>). We used KOBAS software [31] to test the enrichment of DEGs in KEGG pathways.

### 2.5. Validation of RNA-Seq by qRT-PCR

We selected 15 DEGs as experimental validation by quantitative real-time PCR (qRT-PCR), which were performed with three biological and three technical replicates for each cDNA sample. The primers for these genes were designed with NCBI primer-BLAST (Table S1). Reverse transcription was conducted with the GoScript™ Reverse Transcription System (Promega, Madison, WI, USA). We conducted qRT-PCR in a 7500 fast Real-Time PCR system (Applied Biosystems, CA, MA, USA), and analyzed results with the  $\Delta\Delta C_t$  method, and *Pgactin* (F: ATCCTCCGTCTTGACCTTG, R: TGTCCGTCAGGCAACTCAT) gene was used as a reference gene. Each reaction was carried out in a final volume of 20  $\mu$ L, containing 7.5  $\mu$ L of ddH<sub>2</sub>O, 10  $\mu$ L of SYBR Green PCR master mix, 0.5  $\mu$ L of each gene-specific primer and 2  $\mu$ L of diluted cDNA. The PCR thermal cycling conditions were as follows: 95 °C for 10 min; 40 cycles of 95 °C for 5 s, 60 °C for 30 s and 72 °C for 30 s. Data were collected during the extension step: 95 °C for 15 s, 60 °C for 1 min, 95 °C for 30 s and 60 °C for 15 s.

## 3. Results

### 3.1. Overview of Sequencing and Mapping

To obtain a global overview of the salt-induced changes at whole-transcriptomic scale in pomegranate, we constructed 18 cDNA libraries from the roots and leaves of 0 (controls), 3 and 6 days after 200 mM NaCl treatment. A high correlation ( $R^2 > 0.80$ ) between biological replicates was observed for all treatments (Figure S2), which indicated that the biological replicates were reliable in this study. In totally, sequencing libraries yielded 519.47 million reads with 150 bp for both paired ends. After adapter removal and refining, we obtained 155.84 Gb of clean data, and Q30 percentage were all above 90.08% (Table 1). The ratios of reads mapping to the pomegranate genome were high, with values ranging from 93.61% to 95.33%. Then, the unique-mapped reads were 91.89–93.79% and the mapped sequences in genome exon regions were 62.88–69.32% (Table 1). Finally, we assembled 29,226 transcripts from the 18 cDNA libraries of pomegranate roots and leaves under salt stress. To splice the genes more completely and accurately, the StringTie software was employed to reconstruct the transcripts, and then retrieved 34,047 assemblies, including 5396 novel transcripts. Finally, 26,444 genes (including 2421 new genes) were assembled from annotated genes using 7 different databases (see methods), and can be used as a reference of pomegranate genome annotation (Table S2).

**Table 1.** Summary of RNA-Seq results and the alignments in pomegranate genome.

Tissues	Samples ID	Read Number (M)	Base Number (M)	GC Content (%)	Q30 (%)	Mapped Reads (%)	Unique Alignments (%)	Mapped to Exonic (%)
Root (CK)	T01	31,493,153	9,447,945,900	50.43	91.10	94.06	92.27	66.54
	T02	28,438,357	8,531,507,100	50.10	91.78	94.53	92.76	66.84
	T03	26,939,697	8,081,909,100	50.03	91.27	94.99	93.33	62.88
Leaf (CK)	T04	33,023,098	9,906,929,400	52.08	91.22	95.19	93.59	69.32
	T05	27,023,343	8,107,002,900	51.60	90.70	94.88	93.34	68.26
	T06	25,709,176	7,712,752,800	51.48	91.84	95.21	93.54	68.57
Root (3 d)	T07	31,433,566	9,430,069,800	49.95	91.16	94.46	92.67	66.13
	T08	28,144,078	8,443,223,400	50.16	91.23	94.12	92.32	67.30
	T09	26,542,339	7,962,701,700	50.51	91.32	94.63	92.88	67.69

Table 1. Cont.

Tissues	Samples ID	Read Number (M)	Base Number (M)	GC Content (%)	Q30 (%)	Mapped Reads (%)	Unique Alignments (%)	Mapped to Exonic (%)
Leaf (3 d)	T10	28,771,523	8,631,456,900	51.83	91.24	94.97	93.36	68.38
	T11	29,759,918	8,927,975,400	51.32	91.46	95.33	93.79	68.04
	T12	31,628,291	9,488,487,300	51.18	90.08	94.91	93.03	67.80
Root (6 d)	T13	31,761,056	9,528,316,800	50.56	91.91	93.73	91.89	66.87
	T14	29,807,151	8,942,145,300	50.07	91.40	93.89	92.01	66.11
	T15	25,298,243	7,589,472,900	50.29	91.46	93.61	91.89	66.33
Leaf (6 d)	T16	30,075,932	9,022,779,600	51.41	90.84	95.35	93.79	68.50
	T17	27,643,746	8,293,123,800	51.37	91.18	95.18	93.63	68.38
	T18	25,980,948	7,794,284,400	50.88	91.38	94.32	92.66	67.57
Total	—	519,473,615	155,842,084,500	—	—	—	—	—

Reads Number: total Number of paid-end reads in Clean Data; Base Number: total number of bases in Clean Data; Q30%: the ratio of nucleotides with quality value  $\geq 30$ ; GC content: The ratio of guanidine and cytosine nucleotides; Mapped ratio: The percentage of Mapped Reads in proportion of Clean reads.

### 3.2. Identification and Annotation of DEGs

A total of 2255 DEGs were identified from salt treatments with  $FDR < 0.05$  and  $|\log_2(\text{fold change})| \geq 1$ , including 1080 up-regulated and 1175 down-regulated genes, and more DEGs were found in roots (1623 genes) than in leaves (632 genes) (Table S2). To provide insights into the underlying functions of pomegranate transcripts under salt stress, DEGs were annotated after they were compared to well-studied sequences in the GO, Nr, Swiss-Prot, KEGG, and KOG databases (Table S2). In this study, most of DEGs in T1R were distributed in T subgroup (Signal transduction mechanisms), E subgroup (Amino acid transport and metabolism) and G subgroup (Carbohydrate transport and metabolism) (Figure 1a). DEGs of T2R and T1L samples were mostly concentrated in R subgroup (General function prediction only), Q subgroup (Secondary metabolites biosynthesis, transport and catabolism), and K subgroup (Transcription) (Figure 1b,c). The DEGs in T2L were distributed in O subgroup (Posttranslational modification, protein turnover and chaperones), P (Inorganic ion transport and metabolisms) and Q subgroup (Secondary metabolites biosynthesis, transport and catabolism) (Figure 1d). These subgroups were close to the metabolism, such as DNA transcription, cell division, protein modification and energy conversion.

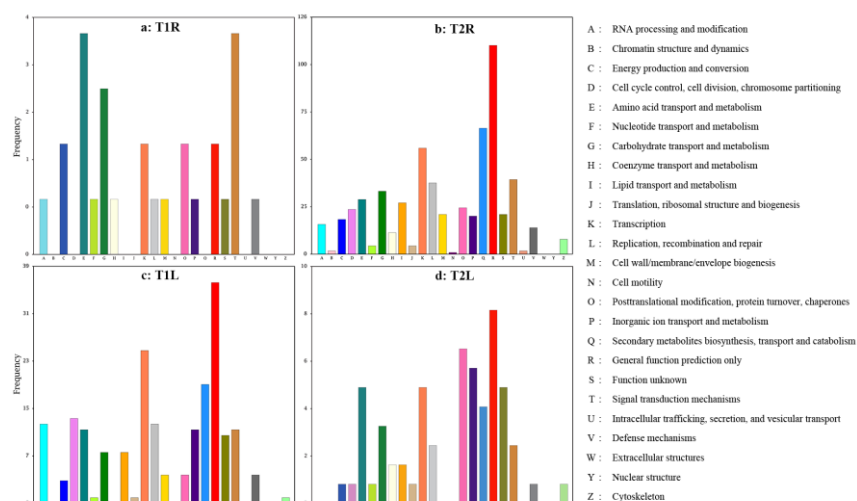


**Figure 1.** COG classification of differentially expressed genes (DEGs) in pomegranate roots and leaves. DEGs enrichments in T1R (a), T2R (b), T1L (c) and T2L (d).

The DEGs of roots and leaves were also analyzed by KEGG pathways enrichment. These pathways were mainly classified into 5 categories (Figure S3) and showed the top 20 pathways (Figure 2). The

majority of pathways in pomegranate roots and leaves were associated with metabolisms, such as global and overview maps, amino acid metabolism, carbohydrate metabolism, lipid metabolism, and energy metabolism, etc. (Figure S3). The metabolism-related genes were significantly enriched in metabolic pathways (ko01100), biosynthesis of secondary metabolites (ko01110), cysteine and methionine metabolism (ko00270), phenylpropanoid biosynthesis (ko00940), starch and sucrose metabolism (ko00500), amino sugar and nucleotide sugar metabolism (ko005200) and protein processing in endoplasmic reticulum (ko04141) pathways. Also, there were some DEGs involved in environmental adaptation (plant-pathogen interaction, ko04626) and signal transduction (plant hormone signal transduction, ko04075) pathways (Figure 2; Figure S3). Genes clustered in genetic information processing were enriched in folding, sorting and degradation, replication and repair, transcription and translation, including protein processing in endoplasmic reticulum (ko04141), DNA replication (ko03030), RNA polymerase (ko03020), RNA transport (ko03013) and RNA degradation (ko03018). In addition, genes involved in the photosynthetic pathways, such as carotenoid biosynthesis (ko00906), porphyrin and chlorophyll metabolism (ko00860) and photosynthesis-antenna proteins (ko00196) were suppressed by salinity.

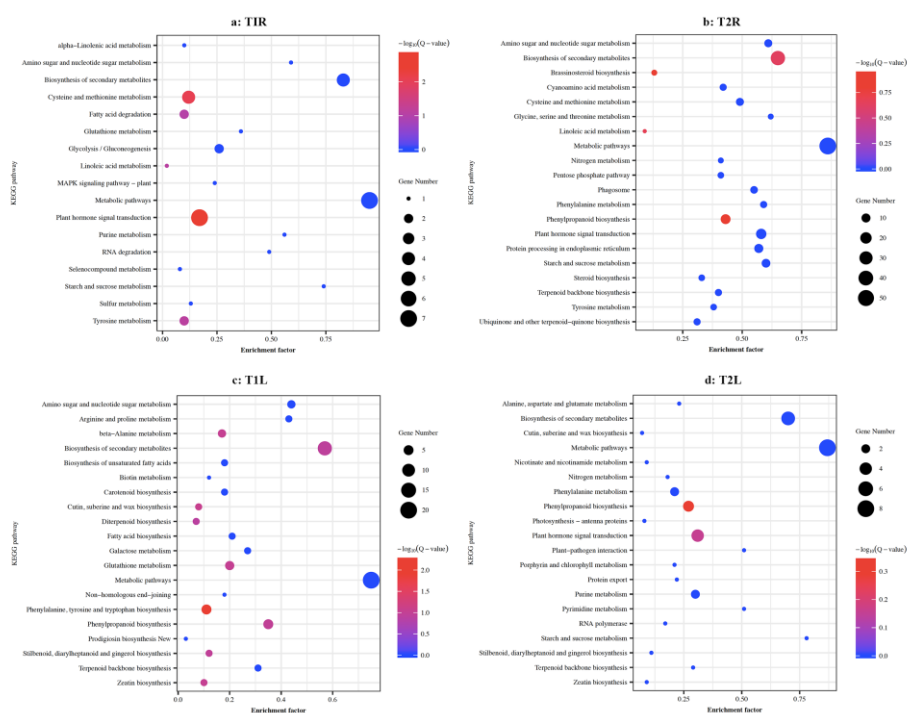


**Figure 2.** The top 20 KEGG pathway of DEGs in pomegranate root and leaf. The horizontal axis showed an enrichment factor, the smaller the enrichment factor is the more significant enrichment of DEGs in this pathway. While the vertical axis illustrated the KEGG pathway, and the color illustrated the  $-\log(Q\text{-value})$ , red color is more reliable and significance enrichment in this pathway. The size of black spots showed the number of DEGs enriched into each pathway. DEGs enrichments in T1R (a), T2R (b), T1L (c), and T2L (d).

### 3.3. The Expressional Patterns of DEGs

Numbers of DEGs increased in roots with the duration of salt-stress, which were opposite in leaves. The genes were both with little overlap in roots and leaves at two points of stress time (Figure 3a). Only a small portion (2.0%) of DEGs (20 up-regulated and 24 down-regulated) shared the common expression tendency between roots and leaves, and even less (1.2%) DEGs showed an utterly opposite tendency between two tissues (3) genes were up-regulated in leaves and down-regulated in roots, 23 genes were down-regulated in leaves but up-regulated in roots) (Figure 3b). The remaining majority of DEGs were exclusively up-regulated or down-regulated in either tissue. Almost 85.9%



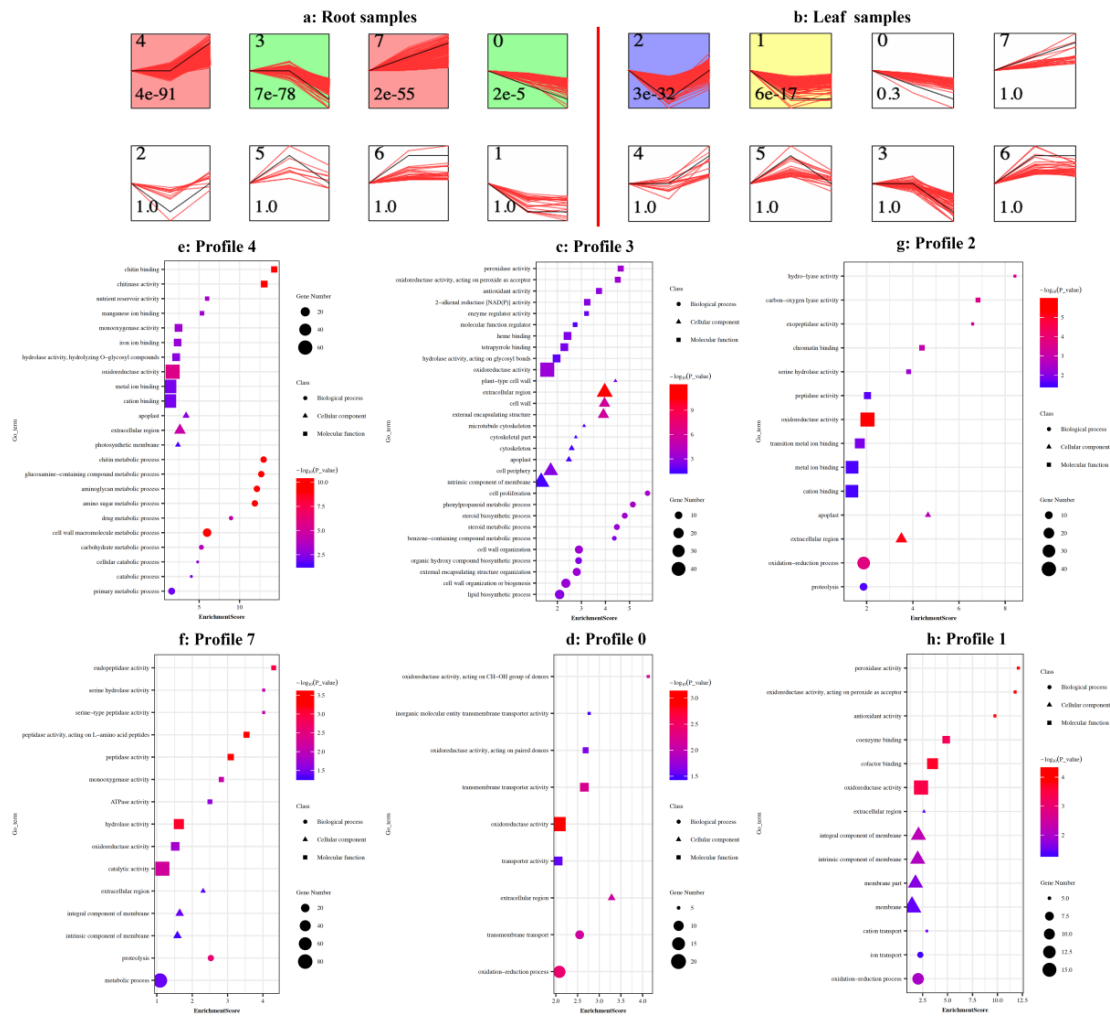


**Figure 4.** The expression patterns of DEGs in pomegranate roots and leaves under NaCl stress using STEM. The P-value in roots; (a) and leaves (b) are shown. The trends of each pattern showed in black lines and the clustered genes are shown in red lines. GO enrichments of Profile 4 (c), Profile 7 (d) Profile 3 (e) and Profile 0 (f) in root libraries (T0R, T1R and T2R); and Profile 2 (g) and Profile 1 (h) in leaf libraries (T0L, T1L and T2L).

Next, DEGs within these profiles were subjected to GO-term enrichment analysis. They were classified into three main categories, including cellular component, biological process, and molecular function, and the top 30 sub-categories (if more than 30,  $p$ -value < 0.05) of each category were shown (Figure 4). In roots, genes in up-regulated pattern of Profile 4 were just induced in T2R. They were enriched in chitinase activity, chitin binding, oxidoreductase activity, metal ion, and cation binding under molecular function; chitin, glucosamine-containing compound, aminoglycan, amino sugar and cell wall macromolecule metabolic process under biological process (Figure 4c; Table S3). Gens were continuously suppressed with the extension of stress in Profile 7, and they were enriched in endopeptidase activity, peptidase activity, hydrolase activity, and catalytic activity under molecular function and proteolysis and metabolic process under biological process (Figure 4d; Table S3). The top subcategories of down-regulated pattern (Profile 3) were extracellular region (GO:0005576), cell wall (GO:0005618) and external encapsulating structure (GO:0030312) under cellular component, and lipid biosynthetic process (GO:0008610), cell wall organization (GO:0071555), and external encapsulating structure organization (GO:0045229) under biological process. (Figure 4e; Table S4). Many DEGs coding cell wall components were mostly suppressed in T2R samples, including four extensins, two pectin acetyltransferase, three polygalacturonase, and three xyloglucan endotransglucosylase/hydrolase

proteins. At the same time, transmembrane transport (GO:0055085) and oxidation-reduction process (GO:0055114) in Profile 0 were inhibited under salt stress. Many genes were identified in these biological process, such as adenine/guanine permease, aquaporin, cationic amino acid transporter, sugar carrier, and zinc transporter (Figure 4f; Table S4). Profile 2 showed a first down- and then up-regulated pattern in leaves, there were many subcategories, such as proteolysis and oxidation-reduction process under biological process, oxidoreductase activity, metal ion, and cation binding under molecular function. The top subcategories in down-regulated pattern of Profile 1 were coenzyme binding, cofactor binding and oxidoreductase activity under molecular function, and oxidation-reduction process, cation and ion transport under biological process. We identified genes coding ion transporters, such as cation/calcium exchanger, zinc transporter, ammonium transporter 1 member, copper-transporting ATPase, potassium transporter (Figure 4h; Table S5).

### 3.4. ABA Signaling Pathway

The ABA signaling pathway mainly consists of three protein classes: ABA receptors (PYR/PYL/RCAR), type 2C protein phosphatase (PP2Cs) and sucrose non-fermenting1-related protein kinase 2 (SnRK2s). In our study, three ABA receptors, *PYLs*, were significantly down-regulated (Figure 5), while 13 *PP2Cs* have different expressional patterns in pomegranate roots and leaves under salt stress. Among these genes, seven *PP2Cs* were up-regulated in roots or leaves, five *PP2Cs* down-regulated, and another gene up-regulated in roots and down-regulated in leaves (Figure 5). In contrast, just one *SnRK2* was identified among the DEGs, and it was up-regulated in leaves, which allowed the accumulation of phosphorylated downstream ABFs and activation of ABA-response genes.

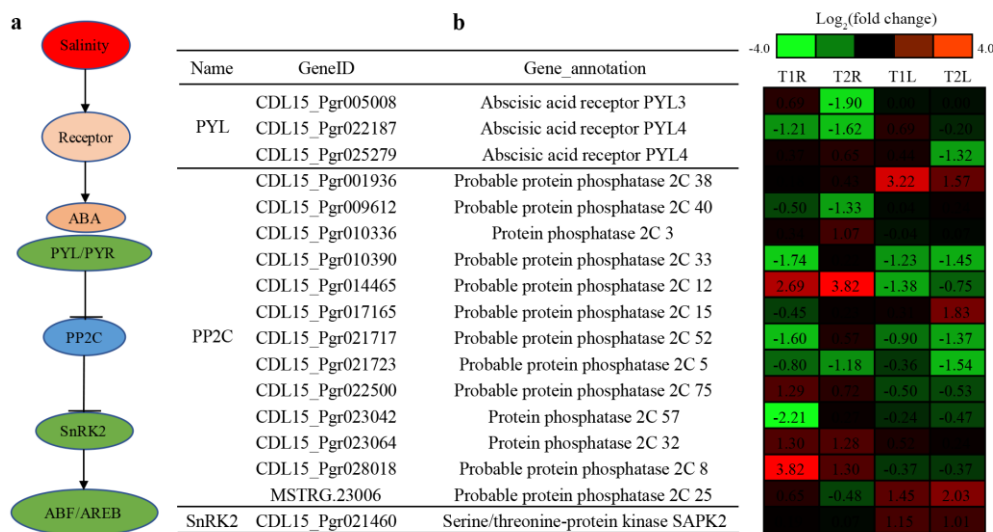


**Figure 5.** DEGs involved in ABA signal transduction pathway in pomegranate under salt stress. (a) ABA signal transduction pathway; (b) DEGs annotations and expressional levels. The color represents with log<sub>2</sub>(fold change), the DEGs with log<sub>2</sub>FC ≥ 1 were up-regulated (red) and log<sub>2</sub>FC ≤ 1 were down-regulated (green) (FDR < 0.05).

### 3.5. Ca<sup>2+</sup>-Related Signaling Pathways

Thirty DEGs involved in Ca<sup>2+</sup>-related signaling pathway were identified, these transcripts coded function proteins included three Ca<sup>2+</sup>-ATPases (ACAs), four cation/H<sup>+</sup> antiporters (CAXs), two cation/calcium exchangers (CCXs), four glutamate receptor (GLRs), ten calcium-binding proteins (CaM/CMLs), two CBL-interacting protein kinases (CIPKs) and five calcium-dependent protein kinases (CDPKs) (Figure 6). Expectedly, two ACAs were up-regulated in roots (T2R), and one was down-regulated in leaves (Figure 6). Ten CAXs expressed differently, including two CAXs located on vacuoles were both up-regulated in T2R. Two CIPKs were significantly up-regulated in leaves,

but no obvious change was observed in roots. The majority of *CaM/CMLs* were up-regulated in roots and down-regulated in leaves. The *CDPKs* were up- or down-regulated in roots and/or leaves. Also, two DEGs, that were involved in the MAPK signaling pathway were identified, and both were down-regulated in leaves (Figure 6).

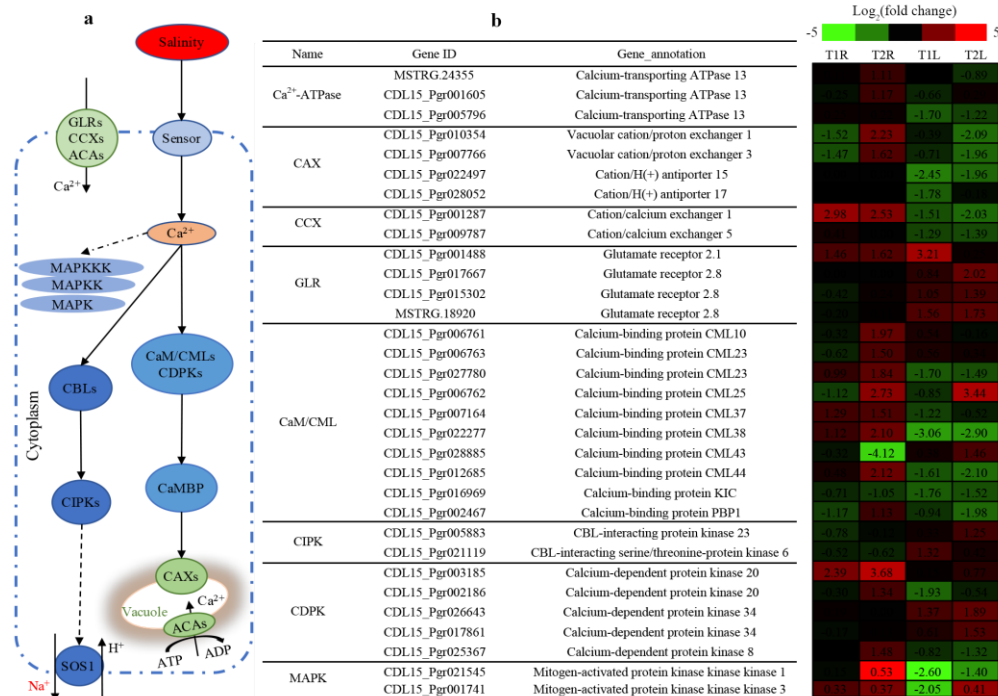


**Figure 6.** The DEGs involved in the Ca<sup>2+</sup>-related signal transduction pathways. (a) Ca<sup>2+</sup>-related signal transduction pathway; (b) DEGs annotations and expressional levels. The color represents with log<sub>2</sub>(fold change), the DEGs with log<sub>2</sub>FC ≥ 1 were up-regulated (red) and log<sub>2</sub>FC ≤ 1 were down-regulated (green) (FDR < 0.05).

### 3.6. The Transcription Factors (TFs)

For identification of the TFs in pomegranate transcriptome, all the mapped genes were analyzed by BLAST against the Plant Transcription Factor Database (PlantTFDB, <http://planttfdb.cbi.pku.edu.cn>). A total of 1346 TFs that were classified into 55 putative families (Table S6). Among these TFs, twenty-seven TF families, including 151 genes expressed differently under salt stress compared to controls. The most abundant of differential expression TFs included NAC, ERF, MYB-related, C2H2, MYB, bHLH, GRAS, WRKY, LBD, B3 and bZIP family genes (Table 2; Table S6).

Under NaCl stress, we found that 12 of 19 NAC genes were up-regulated, and 10 of 19 genes were down-regulated in leaves or roots of pomegranate plants. Interestingly, we also observed that 18 PgNACs significantly changed in T2R when compared to controls, and 4 genes were up-regulated or down-regulated in roots, but reversed in leaves (Table 2; Table S6). These results suggested that many NACs were involved in salt stress, but there were different potential responding mechanisms of NAC domain genes to salinity. Thirteen MYB genes were induced by salt treatment in pomegranate (Table 2). Among these genes, six in roots and four in leaves were up-regulated, and four in roots and eight in leaves were down-regulated. Moreover, sixteen MYB-related genes were detected in our RNA-Seq analyses, thirteen genes were down-regulated, and seven genes were up-regulated by salt stress (Table 2; Table S6). But so far, little was reported that the MYB-related type proteins are related with the responses to salt stress.

**Table 2.** The different expressional TFs in pomegranate under NaCl stress.

TFs	Total No.	DEGs	T1R		T2R		T1L		T2L	
			Up	Down	Up	Down	Up	Down	Up	Down
NAC	97	19	1	1	12	6	1	2	1	4
ERF	114	19	1	1	8	5	1	7		9
MYB_related	91	16	-	-	4	3	1	11	3	2
C2H2	91	13	-	-	8	3	-	1		2
MYB	79	13	-	1	6	4	-	8	4	2
bHLH	102	11	-	1	2	5	1	4	1	1
GRAS	50	9	1	-	9	-	-	-	-	-
LBD	38	7	2	2	2	2	-	2	-	1
WRKY	66	7	-	-	5	-	-	2	1	3
B3	49	3	-	-	1	1	-	1		1
bZIP	45	3	-	-	1	2	-	1	1	1
AP2	8	3	-	-	-	3	-	-	-	-
G2-like	40	3	-	-	1	1	-	-	-	1
HD-ZIP	36	3	-	-	-	2	-	-	-	1
HSF	21	3	-	-	3	-	-	-	-	-
Others	419	19	-	-	8	3	-	6	1	3
Total	1346	151	5	6	70	40	6	46	13	31

The AP2/ERF superfamily is divided into three families: the AP2 family proteins containing two repeated AP2/ERF domains, the ERF family proteins, containing a single AP2/ERF domain, and the RAV family proteins containing a B3 domain. There were 19 *PgERFs*, and 3 *PgAP2s* significantly expressed in treatments when compared to controls (Table 2). Fifteen *ERFs* were down-regulated, and all of *AP2* were repressed by salinity. There were 9 up-regulated and 8 down-regulated *C2H2*, three up-regulated and nine down-regulated *bHLH*, five up-regulated and three down-regulated *WRKY* identified in pomegranate roots and leaves. Remarkably, nine *GRASs* were up-regulated in the root, but the no-significant change in leaves (Table 2; Table S6).

### 3.7. qRT-PCR Validation

To confirm the reliability of the expression levels obtained from the RNA-Seq, fifteen DEGs, including five *PgERFs*, three *PgMYBs* and seven *PgNACs* were selected for qRT-PCR assays. The results showed that the expression level of each transcript closely corresponded to the transcript level estimated from the sequence data with  $R^2 \geq 0.85$  (Figure 7), which implies reproducibility and accuracy of the RNA-Seq results.

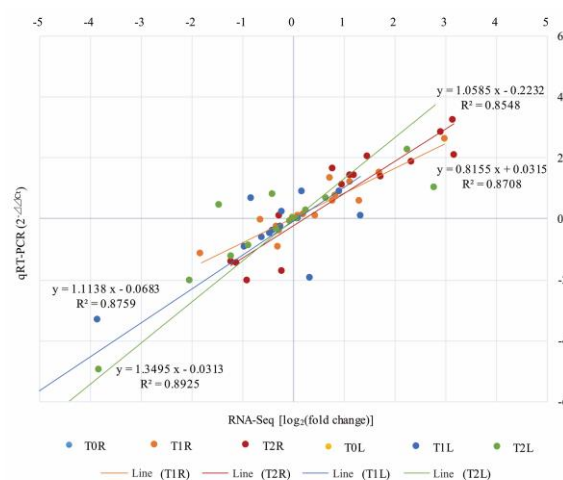


**Figure 7.** The relationship between qRT-PCR and RNA-Seq data. The color circle is gene expression level. The lines represent co-relationship with dependent linear equations.

#### 4. Discussion

RNA-sequencing techniques have proven to be beneficial and economical for scanning the transcribed genes, both in model and non-model plant species. In this study, we used the RNA-Seq approach as a powerful tool to elucidate the molecular responses to salt stress in pomegranate. Finally, we reconstructed the transcripts and identified 5396 novel genes from the 18 cDNA libraries. There were significant differences between the percentage of total mapped reads and the mapped reads in exonic regions. Theoretically, the ratio of sequencing reads that produced from mature mRNA mapped into exonic regions could be 100%. However, a portion of 30.68–37.12% reads were also mapped into intronic and intergenic regions for the following reasons: (1) The coding and non-coding sequences in the reference genome might have been annotated incorrectly; (2) the new alternative splicing (SNPs) and novel genes resulted from the alternative mRNA splicing and transcripts reconstructing; (3) variations exist between sequencing and reference genome genotypes, which are attributed to the gaps and diversity of their sequences [32,33].

Under salt stress, plants firstly experience osmotic stress due to a disorder of water uptake. Then a process of gradual recovery due to the partially or completely re-established uptake of water occurs within days after the salt treatment [34,35]. We identified 2255 DEGs through the 18 mRNA libraries. From the third to sixth day after treatment, there were significant differences between pomegranate roots and leaves, with little overlap of DEGs responding salinity (Figure 3). More salt-related genes were up-regulated in roots, while the majority of suppressed genes recovered with salt-treating process in leaves. In contrast, the osmotic adjustment of leaves started only after roots had reached new water equilibrium [36]. These tissue-specific and time-specific differences between roots and leaves have also been reported in *Arabidopsis thaliana* (L.) [37], *Populus euphratica* (Oliv.) [36], and *Millettia pinnata* (L.) [38]. Many DEGs were involved in down-regulated patterns in roots, such as cell wall organization, transmembrane transport and oxidation-reduction process, but the proteolysis and metabolic process were over-expressed. Otherwise, most of DEGs involved in oxidation-reduction process and ion transport in leaves were suppressed (Figure 4). The cell wall plays an important role in protecting plant from salt toxicity [39]. In our study, extensin, pectin acetyltransferase, polygalacturonase, and xyloglucan endotransglucosylase/hydrolase proteins were identified in roots (Table S4). These proteins are important components of the cell wall, which affect plant growth by mediating cell enlargement and expansion [39]. Many DEGs involved in transmembrane transport code for various channels, carriers and pumps, and ion transporters, such as aquaporin, cationic amino acid transporter, sugar carrier, and zinc transporter (Table S4). They worked together to transport coenzymes, amino acids, carbohydrates, and ions under salt stress. The suppressed genes coding proteins, such as dehydrogenase, cytochrome P450s and peroxidase involved in oxidation-reduction process, play essential roles in responding to salinity [40,41] (Tables S4 and S5). These results indicated that salinity affected pomegranate growth and development by inhibiting the cell division and transmembrane transport, as well as slowing down the redox reactions.

On the other hand, over-represented genes in roots were enriched in metabolic process, carbohydrate metabolic process, and catabolic process, etc. These metabolism-related genes in roots were also enriched in KEGG pathways, such as metabolic pathways (ko01100), biosynthesis of secondary metabolites (ko01110), phenylpropanoid biosynthesis (ko00940), starch and sucrose metabolism (ko00500), amino sugar and nucleotide sugar metabolism (ko005200) (Figure 2; Table S3). The carbohydrates such as glycan, starch, sucrose, amino sugar have been demonstrated as osmolytes and energy resources in plant responses to salt stress, especially in halophyte species [42]. The accelerated metabolisms in pomegranate might contribute to its adaptation responses to salt stress. Similar expression patterns of metabolism-related genes were observed in *Oryza sativa* (L.) [43], *Thellungiella halophila* (C. A. Mey.) [42] and *Helianthus tuberosus* (L.) [44] under salt stress. Metal ions/cations, such as  $K^+$ ,  $Ca^{2+}$ ,  $Mg^{2+}$ ,  $Fe^{2+}$ ,  $Cu^{2+}$ , and  $Zn^{2+}$ , act as cofactors participating in the catalytic activity of the enzymes they bind to [44]. The up-regulated DEGs involved in metal ion/cation binding might accelerate the catalytic activity. At the same time, the ion transport process was inhibited in roots and leaves (Tables

S3 and S5). The restriction of ion transport indicated that the excess of  $\text{Na}^+$  inhibited the uptake of mineral ions [4]. The results correspond to the physiological responses in other pomegranate cultivars under salt stress [45]. We suspected that pomegranate could cope with the toxic ions to some extent via decreasing uptake of ions from soil and increasing utilization of ions in cells. The toxic ions access into the leaf cells with the transpiration, but the detrimental effect is a slow process taking weeks or months, eventually cause salt toxicity in leaves [46]. Plants were only exposed to salinity stress just for six days in our research, so further study is needed to reveal the long-term effect of salinity.

ABA is a critical hormone, which regulates plant growth, development, as well as responses to environmental stresses such as salinity, drought, heat, cold, wound, and pathogen [47,48]. Once ABA is produced, ABA-bound receptors bind ABA, inhibit *PP2Cs*, such as *ABI1* and *ABI2*, thereby activate *SnRK2s* [49]. The *SnRK2s* are involved in plant responses to abiotic stresses, which can phosphorylate the ABA-responsive element binding factor (ABF) and trigger the expression of ABA-responsive genes [50]. In our study, three ABA receptors, *PYLs*, were significantly down-regulated in roots or leaves (Figure 5), which is consistent with results in tea (*Camellia sinensis* L.) [51] and grape (*Vitis vinifera* L.) [52]. The down-regulation of *PYLs* can reduce plant sensitivity to ABA in response to salt stress and help plants adapt to salinity. The expressional differences of *PP2Cs* between roots and leaves in pomegranate are similar to other plants, which indicate that *PP2Cs* may participate in response to salinity via different strategies [52,53]. *PYR/PYLs* may regulate *SnRK2s* directly or indirectly, however, whether *SnRK2s* responding to various abiotic stresses in an ABA-independent or ABA-dependent pathway needs further investigation.

$\text{Ca}^{2+}$  referred as a second messenger plays a very important role in many stress-related signaling transduction pathways. Under various abiotic stresses, over-accumulation of ions induce a temporary fluctuations in plant cytosolic ( $[\text{Ca}^{2+}]_{\text{cyt}}$ ) levels [54]. The genes involved in CIPKs and CDPKs pathways, such as *ACAs*, *CAXs*, *GLRs*, *CaM/CMLs*, *CBLs* etc., participate in transporting and binding  $\text{Ca}^{2+}$ , sensing and relaying signals in plant cell under salinity stress [55,56]. In our study, we found two *ACAs* and two *CAXs* located on vacuoles were up-regulated in T2R, and the majority of *CaM/CMLs* were up-regulated in roots but down-regulated in leaves (Figure 6). Previous reports revealed a central role for CaMs in the regulation of  $\text{Ca}^{2+}$  channels and pumps, like CNGCs and *ACAs* [57,58]. The negative effect of CaM on CNGC activity provides a direct feedback pathway to restrict the influx of  $\text{Ca}^{2+}$  into plant cells [58]. The CaM stimulates the activity of these *ACAs* by preventing their auto-inhibition [58]. Collectively, under salt stress, pomegranate plants restrain the excess influx of  $\text{Ca}^{2+}$  into root cells under salinity. Meanwhile, it coped with the excess  $\text{Ca}^{2+}$  via removing  $\text{Ca}^{2+}$  from the cytosol by *ACAs* and *CAXs* in plasma membrane, including efflux of excess  $\text{Ca}^{2+}$  into the outer rhizosphere and/or the influx into vacuoles [59,60].

Specifically, transcription factors, such as NAC, MYB, AP2/ERF, bHLH, WRKY, GRAS family genes, regulated the expression of downstream genes to cope with various stresses [17]. Our study indicated that the TFs of pomegranate participated in the response to salinity with different patterns. For example, most of *NAC* and *C2H2* genes were up-regulated in roots, while most of *MYB* and *MYB-related* genes were down-regulated in leaves (Table 2; Table S6). Interestingly, nine *GRASs* were all up-regulated in T2R, which is mainly due to that these proteins play roles in plant development, including root development, axillary shoot development, and maintenance of the shoot apical meristem [61]. We also found 57 DEGs coding for salt-induced effectors, including two *SODs*, two *APXs*, nineteen *PODs*, five *LEAs*, five *AQPs*, ten *HSFs*, three *AKTs*, and one *HKT* (Table S7). Two *APXs* were up-regulated and two *SODs* were down-regulated in leaves. Fourteen and nine *PODs* were suppressed in roots and leaves, respectively. Most of *AQPs* (4 of 5) were down-regulated, while all of *LEAs* (5 of 5) and majority of *HSFs* (9 of 10) were up-regulated in pomegranate tissues under salt stress. *LEAs* and *HSPs* were reported to prevent protein denaturation and maintain cell membrane fluidity under stress [62]. Then the DEGs of *LEA* and *HSF* in pomegranate contributed to mitigating salt stress. The expressions of three *AKTs* and one *HKT* were significantly down-regulated, which suggested that the influxes of  $\text{K}^+$  and  $\text{Na}^+$  in the cell were restricted [63].

Briefly, when pomegranate plants are exposed to high salinity, Na<sup>+</sup> enters the cell and simultaneously generates stress signals. The messengers Ca<sup>2+</sup>, ROSs (reactive oxygen species), and ABA transduced the signals, and then the cascades, including Ca<sup>2+</sup>-sensors, MAPK cascades and TFs, involved in secondary and tertiary regulatory networks were activated (Figure S4). TFs regulated the expression of downstream functional genes, such as *HSPs*, *LEAs*, *AQPs*, *SODs*, and *APXs*, to cope with salt stress.

## 5. Conclusions

In summary, our research sheds light on the pomegranate molecular response mechanisms to salinity. The differentially expressed genes could also provide references for selecting salt-tolerant breeding materials in pomegranate breeding processes.

**Accession Codes:** The raw data were deposited in NCBI Sequence Read Archive (SRA) database (<http://www.ncbi.nlm.nih.gov/Traces/sra>) under accession number SRP148507.

**Supplementary Materials:** The following are available online at <http://www.mdpi.com/2073-4395/10/1/44/s1>, Figure S1: The images of untreated and treated plants. Figure S2: Pearson correlation of all samples, Figure S3: Pathways classification into cellular process, environmental information processing, genetic processing, metabolism and organismal system based on the KEGG analysis, Figure S4: Signaling networks in pomegranate under salt stress, Table S1: The primers used for qPCR validation of 15 DEGs, Table S2: Total numbers of DEGs assigned to databases, Table S3: DEGs involved in up-regulated patterns of pomegranate roots, Table S4: DEGs involved in down-regulated patterns of pomegranate roots, Table S5: DEGs involved in expressional patterns of pomegranate leaves, Table S6: The numbers of differently expressed TFs in pomegranate under NaCl stress, Table S7: The salt-induced DEGs in pomegranate under NaCl stress.

**Author Contributions:** Conceptualization, C.L. and Y.Z.; methodology, C.L. and Y.Z.; formal analysis, C.L., Y.Z., J.W., and X.Z.; investigation, C.L., Y.Z., X.Z., and J.W.; writing—original draft preparation, C.L.; writing—review and editing, C.L., X.Z., M.G., and Z.Y.; supervision, M.G. and Z.Y.; Funding acquisition, Z.Y. All authors have read and agreed to the published version of the manuscript.

**Funding:** This work was supported by the Initiative Project for Talents of Nanjing Forestry University (GXL2014070, GXL2018032), the Natural Science Foundation of Jiangsu Province (BK20180768), the Doctorate Fellowship Foundation of Nanjing Forestry University, and the Priority Academic Program Development of Jiangsu High Education Institutions (PAPD).

**Conflicts of Interest:** The authors declare no conflict of interest.

## References

- Li, J.; Pu, L.; Zhu, M.; Zhang, R. The present situation and hot issues in the salt-affected soil research. *Acta Geogr. Sin.* **2012**, *67*, 1233–1245.
- Zhu, J.K. Plant salt tolerance. *Trends Plant Sci.* **2001**, *6*, 66–71. [[CrossRef](#)]
- Pandey, P.; Ramegowda, V.; Senthil-Kumar, M. Shared and unique responses of plants to multiple individual stresses and stress combinations: Physiological and molecular mechanisms. *Front. Plant Sci.* **2015**, *6*, 723. [[CrossRef](#)]
- Munns, R.; Tester, M. Mechanisms of salinity tolerance. *Annu. Rev. Plant Biol.* **2008**, *59*, 651–681. [[CrossRef](#)]
- Zhang, H.; Han, B.; Wang, T.; Chen, S.; Li, H.; Zhang, Y.; Dai, S. Mechanisms of plant salt response: Insights from proteomics. *J. Proteome Res.* **2011**, *11*, 49–67. [[CrossRef](#)]
- Bui, E.N. Soil salinity: A neglected factor in plant ecology and biogeography. *J. Arid Environ.* **2013**, *92*, 14–25. [[CrossRef](#)]
- Apse, M.P.; Blumwald, E. Na<sup>+</sup> transport in plants. *FEBS Lett.* **2007**, *581*, 2247–2254. [[CrossRef](#)]
- Munns, R.; James, R.A.; Gilliam, M.; Flowers, T.J.; Colmer, T.D. Tissue tolerance: An essential but elusive trait for salt-tolerant crops. *Funct. Plant Biol.* **2016**, *43*, 1103–1113. [[CrossRef](#)]
- Attia, H.; Karray, N.; Msilini, N.; Lachaâl, M. Effect of salt stress on gene expression of superoxide dismutases and copper chaperone in *Arabidopsis thaliana*. *Biol. Plant.* **2011**, *55*, 159–163. [[CrossRef](#)]
- Shafi, A.; Chauhan, R.; Gill, T.; Swarnkar, M.K.; Sreenivasulu, Y.; Kumar, S.; Kumar, N.; Shankar, R.; Ahuja, P.S.; Singh, A.K. Expression of *SOD* and *APX* genes positively regulates secondary cell wall biosynthesis and promotes plant growth and yield in *Arabidopsis* under salt stress. *Plant Mol. Biol.* **2015**, *87*, 615–631. [[CrossRef](#)]

11. Kumar, S.; Beena, A.S.; Awana, M.; Singh, A. Salt-induced tissue-specific cytosine methylation downregulates expression of *HKT* genes in contrasting wheat (*Triticum aestivum* L.) genotypes. *DNA Cell Biol.* **2017**, *36*, 283–294. [[CrossRef](#)] [[PubMed](#)]
12. Yokoi, S.; Quintero, F.J.; Cubero, B.; Ruiz, M.T.; Bressan, R.A.; Hasegawa, P.M.; Pardo, J.M. Differential expression and function of *Arabidopsis thaliana* *NHX* Na<sup>+</sup>/H<sup>+</sup> antiporters in the salt stress response. *Plant J.* **2010**, *30*, 529–539. [[CrossRef](#)] [[PubMed](#)]
13. Hu, W.; Yuan, Q.; Wang, Y.; Cai, R.; Deng, X.; Wang, J.; Zhou, S.; Chen, M.; Chen, L.; Huang, C. Overexpression of a wheat aquaporin gene, *TaAQP8*, enhances salt stress tolerance in transgenic tobacco. *Plant Cell Physiol.* **2012**, *53*, 2127–2141. [[CrossRef](#)] [[PubMed](#)]
14. Duan, J.; Cai, W. *OsLEA3-2*, an abiotic stress induced gene of rice plays a key role in salt and drought tolerance. *PLoS ONE* **2012**, *7*, e45117. [[CrossRef](#)]
15. Zhou, A.; Liu, E.; Ma, H.; Feng, S.; Gong, S.; Wang, J. NaCl-induced expression of *AtVHA-c5* gene in the roots plays a role in response of *Arabidopsis* to salt stress. *Plant Cell Rep.* **2018**, *37*, 443–452. [[CrossRef](#)]
16. Hasegawa, P.M.; Bressan, R.A.; Zhu, J.K.; Bohnert, H.J. Plant cellular and molecular responses to high salinity. *Annu. Rev. Plant Physiol. Plant Mol. Biol.* **2000**, *51*, 463–499. [[CrossRef](#)]
17. Deinlein, U.; Stephan, A.B.; Horie, T.; Luo, W.; Xu, G.; Schroeder, J.I. Plant salt-tolerance mechanisms. *Trends Plant Sci.* **2014**, *19*, 371–379. [[CrossRef](#)]
18. Guo, S.M.; Tan, Y.; Chu, H.J.; Sun, M.X.; Xing, J.C. Transcriptome sequencing revealed molecular mechanisms underlying tolerance of *Suaeda salsa* to saline stress. *PLoS ONE* **2019**, *14*, e0219979. [[CrossRef](#)]
19. Yuan, Z.; Fang, Y.; Zhang, T.; Fei, Z.; Han, F.; Liu, C.; Liu, M.; Xiao, W.; Zhang, W.; Wu, S. The pomegranate (*Punica granatum* L.) genome provides insights into fruit quality and ovule developmental biology. *Plant Biotechnol. J.* **2018**, *16*, 1363–1374. [[CrossRef](#)]
20. Silva, J.A.T.D.; Rana, T.S.; Narzary, D.; Verma, N.; Meshram, D.T.; Ranade, S.A. Pomegranate biology and biotechnology: A review. *Sci. Hortic.* **2013**, *160*, 85–107. [[CrossRef](#)]
21. Holl, D.; Hatib, K.; Bar-Ya'akov, I. Pomegranate: Botany, horticulture, breeding. *Hortic. Rev.* **2009**, *35*, 127–191.
22. Karimi, H.R.; Hasanpour, Z. Effects of salinity and water stress on growth and macro nutrients concentration of pomegranate (*Punica granatum* L.). *J. Plant Nutr.* **2014**, *37*, 1937–1951. [[CrossRef](#)]
23. Okhovatianardakani, A.R.; Mehrabianian, M.; Dehghani, F.; Akbarzadeh, A. Salt tolerance evaluation and relative comparison in cuttings of different pomegranate cultivars. *Plant Soil Environ.* **2010**, *56*, 176–185. [[CrossRef](#)]
24. Liu, C.; Yan, M.; Huang, X.; Yuan, Z. Effects of salt stress on growth and physiological characteristics of pomegranate (*Punica granatum* L.) cuttings. *Pak. J. Bot.* **2018**, *50*, 457–464.
25. Feng, Z.T.; Deng, Y.Q.; Fan, H.; Sun, Q.J.; Sui, N.; Wang, B.S. Effects of NaCl stress on the growth and photosynthetic characteristics of *Ulmus pumila* L. seedlings in sand culture. *Photosynthetica* **2014**, *52*, 313–320. [[CrossRef](#)]
26. Patel, R.K.; Jain, M. NGS QC Toolkit: A toolkit for quality control of next generation sequencing data. *PLoS ONE* **2012**, *7*, e30619. [[CrossRef](#)]
27. Kim, D.; Pertea, G.; Trapnell, C.; Pimentel, H.; Kelley, R.; Salzberg, S.L. TopHat2: Accurate alignment of transcriptomes in the presence of insertions, deletions and gene fusions. *Genome Biol.* **2013**, *14*, R36. [[CrossRef](#)]
28. Pertea, M.; Kim, D.; Pertea, G.M.; Leek, J.T.; Salzberg, S.L. Transcript-level expression analysis of RNA-seq experiments with HISAT, StringTie and Ballgown. *Nat. Protoc.* **2016**, *11*, 1650–1667. [[CrossRef](#)]
29. Götz, S.; Garcíagómez, J.M.; Terol, J.; Williams, T.D.; Nagaraj, S.H.; Nueda, M.J.; Robles, M.; Talón, M.; Dopazo, J.; Conesa, A. High-throughput functional annotation and data mining with the Blast2GO suite. *Nucleic Acids Res.* **2008**, *36*, 3420–3435. [[CrossRef](#)]
30. Ernst, J.; Nau, G.J.; Bar-Joseph, Z. Clustering short time series gene expression data. *Bioinformatics* **2005**, *21*, i159–i168. [[CrossRef](#)]
31. Mao, X.; Cai, T.; Olyarchuk, J.G.; Wei, L. Automated genome annotation and pathway identification using the KEGG Orthology (KO) as a controlled vocabulary. *Bioinformatics* **2005**, *21*, 3787–3793. [[CrossRef](#)] [[PubMed](#)]
32. Wang, J.; Zhu, J.; Zhang, Y.; Fan, F.; Li, W.; Wang, F.; Zhong, W.; Wang, C.; Yang, J. Comparative transcriptome analysis reveals molecular response to salinity stress of salt-tolerant and sensitive genotypes of indica rice at seedling stage. *Sci. Rep.* **2018**, *8*, 2085. [[CrossRef](#)] [[PubMed](#)]

33. Zhou, Y.; Yang, P.; Cui, F.; Zhang, F.; Luo, X.; Xie, J. Transcriptome analysis of salt stress responsiveness in the seedlings of Dongxiang wild rice (*Oryza rufipogon* Griff.). *PLoS ONE* **2016**, *11*, e0146242. [[CrossRef](#)]
34. Munns, R.; James, R.A.; Läuchli, A. Approaches to increasing the salt tolerance of wheat and other cereals. *J. Exp. Bot.* **2006**, *57*, 1025–1043. [[CrossRef](#)]
35. Munns, R. Genes and salt tolerance: Bringing them together. *New Phytol.* **2005**, *167*, 645–663. [[CrossRef](#)]
36. Monika, B.; Mikael, B.; Basia, V.; Atef, A.O.; Payam, F.; Dennis, J.; Ottow, E.A.; Cullmann, A.D.; Joachim, S.; Jaakko, K.R. Linking the salt transcriptome with physiological responses of a salt-resistant *Populus* species as a strategy to identify genes important for stress acclimation. *Plant Physiol.* **2010**, *154*, 1697–1709.
37. Ma, S.; Gong, Q.; Bohnert, H.J. Dissecting salt stress pathways. *J. Exp. Bot.* **2006**, *57*, 1097–1107. [[CrossRef](#)]
38. Huang, J.; Xiang, L.; Hao, Y.; Chen, S.; Zhang, W.; Huang, R.; Zheng, Y. Transcriptome characterization and sequencing-based identification of salt-responsive genes in *Millettia pinnata*, a semi-mangrove plant. *DNA Res.* **2012**, *19*, 195–207. [[CrossRef](#)]
39. Le Gall, H.; Philippe, F.; Domon, J.-M.; Gillet, F.; Pelloux, J.; Rayon, C. Cell wall metabolism in response to abiotic stress. *Plants* **2015**, *4*, 112–166. [[CrossRef](#)]
40. Fatehi, F.; Hosseinzadeh, A.; Alizadeh, H.; Brimavandi, T.; Struik, P.C. The proteome response of salt-resistant and salt-sensitive barley genotypes to long-term salinity stress. *Mol. Biol. Rep.* **2012**, *39*, 6387–6397. [[CrossRef](#)]
41. Bushman, B.S.; Amundsen, K.L.; Warnke, S.E.; Robins, J.G.; Johnson, P.G. Transcriptome profiling of Kentucky bluegrass (*Poa pratensis* L.) accessions in response to salt stress. *BMC Genom.* **2016**, *17*, 48. [[CrossRef](#)] [[PubMed](#)]
42. Wang, X.; Chang, L.; Wang, B.; Wang, D.; Li, P.; Wang, L.; Yi, X.; Huang, Q.; Peng, M.; Guo, A. Comparative proteomics of *Thellungiella halophila* leaves from plants subjected to salinity reveals the importance of chloroplastic starch and soluble sugars in halophyte salt tolerance. *Mol. Cell. Proteom.* **2013**, *12*, 2174–2195. [[CrossRef](#)] [[PubMed](#)]
43. Boriboonkaset, T.; Theerawitaya, C.; Yamada, N.; Pichakum, A.; Supaibulwatana, K.; Cha-um, S.; Takabe, T.; Kirdmanee, C. Regulation of some carbohydrate metabolism-related genes, starch and soluble sugar contents, photosynthetic activities and yield attributes of two contrasting rice genotypes subjected to salt stress. *Protoplasma* **2013**, *250*, 1157–1167. [[CrossRef](#)] [[PubMed](#)]
44. Zhang, A.; Han, D.; Wang, Y.; Mu, H.; Zhang, T.; Yan, X.; Pang, Q. Transcriptomic and proteomic feature of salt stress-regulated network in Jerusalem artichoke (*Helianthus tuberosus* L.) root based on de novo assembly sequencing analysis. *Planta* **2018**, *247*, 715–732. [[CrossRef](#)] [[PubMed](#)]
45. Sun, Y.; Niu, G.; Masabni, J.G.; Ganjegunte, G. Relative salt tolerance of 22 pomegranate (*Punica granatum*) cultivars. *HortScience* **2018**, *53*, 1513–1519. [[CrossRef](#)]
46. Aroca, R.; Porcel, R.; Ruiz-Lozano, J.M. Regulation of root water uptake under abiotic stress conditions. *J. Exp. Bot.* **2011**, *63*, 43–57. [[CrossRef](#)] [[PubMed](#)]
47. Finkelstein, R.R.; Gampala, S.S.; Rock, C.D. Abscisic acid signaling in seeds and seedlings. *Plant Cell* **2002**, *14*, S15–S45. [[CrossRef](#)]
48. Shinozaki, K.; Yamaguchi-Shinozaki, K. Molecular responses to dehydration and low temperature: Differences and cross-talk between two stress signaling pathways. *Curr. Opin. Plant Biol.* **2000**, *3*, 217–223. [[CrossRef](#)]
49. Fan, W.; Zhao, M.; Li, S.; Bai, X.; Li, J.; Meng, H.; Mu, Z. Contrasting transcriptional responses of *PYR1/PYL/RCAR* ABA receptors to ABA or dehydration stress between maize seedling leaves and roots. *BMC Plant Biol.* **2016**, *16*, 99. [[CrossRef](#)]
50. Zhang, H.; Li, W.; Mao, X.; Jing, R.; Jia, H. Differential activation of the wheat SnRK2 family by abiotic stresses. *Front. Plant Sci.* **2016**, *7*, 420. [[CrossRef](#)]
51. Wan, S.; Wang, W.; Zhou, T.; Zhang, Y.; Chen, J.; Xiao, B.; Yang, Y.; Yu, Y. Transcriptomic analysis reveals the molecular mechanisms of *Camellia sinensis* in response to salt stress. *Plant Growth Regul.* **2018**, *84*, 481–492. [[CrossRef](#)]
52. Boneh, U.; Biton, I.; Zheng, C.; Schwartz, A.; Ben-Ari, G. Characterization of potential ABA receptors in *Vitis vinifera*. *Plant Cell Rep.* **2012**, *31*, 311–321. [[CrossRef](#)] [[PubMed](#)]
53. Cao, J.; Min, J.; Peng, L.; Chu, Z. Genome-wide identification and evolutionary analyses of the PP2C gene family with their expression profiling in response to multiple stresses in *Brachypodium distachyon*. *BMC Genom.* **2016**, *17*, 175. [[CrossRef](#)] [[PubMed](#)]
54. McCormack, E.; Tsai, Y.-C.; Braam, J. Handling calcium signaling: Arabidopsis *CaMs* and *CMLs*. *Trends Plant Sci.* **2005**, *10*, 383–389. [[CrossRef](#)] [[PubMed](#)]

55. Dang, Z.H.; Zheng, L.L.; Jia, W.; Zhe, G.; Wu, S.B.; Zhi, Q.; Wang, Y.C. Transcriptomic profiling of the salt-stress response in the wild recretohalophyte *Reaumuria trigyna*. *BMC Genom.* **2013**, *14*, 29. [[CrossRef](#)] [[PubMed](#)]
56. Yang, Y.; Zhang, C.; Tang, R.; Xu, H.; Lan, W.; Zhao, F.; Luan, S. Calcineurin B-Like proteins CBL4 and CBL10 mediate two independent salt tolerance pathways in Arabidopsis. *Int. J. Mol. Sci.* **2019**, *20*, 2421. [[CrossRef](#)]
57. Viridi, A.S.; Singh, S.; Singh, P. Abiotic stress responses in plants: Roles of calmodulin-regulated proteins. *Front. Plant Sci.* **2015**, *6*, 809. [[CrossRef](#)]
58. Cheval, C.; Aldon, D.; Galaud, J.-P.; Ranty, B. Calcium/calmodulin-mediated regulation of plant immunity. *Biochim. Biophys. Acta Mol. Cell Res.* **2013**, *1833*, 1766–1771. [[CrossRef](#)]
59. Apse, M.P.; Sottosanto, J.B.; Blumwald, E. Vacuolar cation/H<sup>+</sup> exchange, ion homeostasis, and leaf development are altered in a T-DNA insertional mutant of *AtNHX1*, the Arabidopsis vacuolar Na<sup>+</sup>/H<sup>+</sup> antiporter. *Plant J.* **2010**, *36*, 229–239. [[CrossRef](#)]
60. Huda, K.M.; Banu, M.S.; Tuteja, R.; Tuteja, N. Global calcium transducer P-type Ca<sup>2+</sup>-ATPases open new avenues for agriculture by regulating stress signalling. *J. Exp. Bot.* **2013**, *64*, 3099–3109. [[CrossRef](#)]
61. Bolle, C. The role of GRAS proteins in plant signal transduction and development. *Planta* **2004**, *218*, 683–692. [[CrossRef](#)] [[PubMed](#)]
62. Hoekstra, F.A.; Golovina, E.A.; Buitink, J. Mechanisms of plant desiccation tolerance. *Trends Plant Sci.* **2001**, *6*, 431–438. [[CrossRef](#)]
63. Xu, M.; Chen, C.; Cai, H.; Wu, L. Overexpression of *PeHKT1; 1* Improves Salt Tolerance in Populus. *Genes* **2018**, *9*, 475. [[CrossRef](#)] [[PubMed](#)]



© 2019 by the authors. Licensee MDPI, Basel, Switzerland. This article is an open access article distributed under the terms and conditions of the Creative Commons Attribution (CC BY) license (<http://creativecommons.org/licenses/by/4.0/>).